The Kinetics of the Reaction of H Atoms with C_4F_6

Xiaohua Hu, A. Goumri, and Paul Marshall*

University of North Texas, Department of Chemistry, P.O. Box 305070, Denton, Texas 76203-5070

Received: April 24, 2001; In Final Form: September 13, 2001

The rate constant k for the gas-phase reaction of atomic hydrogen with 1,1,2,3,4,4-hexafluoro-1,3-butadiene has been measured over the temperature range 290−1010 K by time-resolved atomic resonance fluorescence using H_2O and NH_3 as precursors, at argon pressures of about 30−140 mbar. Over the range 290−620 K a positive activation energy was observed, $k = (3.40 \pm 0.34) \times 10^{-11}$ exp[(−16.7 ± 0.4) kJ mol^{-1}/RT] cm^3 molecule^{-1} s^{-1}, and k dropped rapidly between 620 and 700 K. Over the range 700−1010 K, $k = (1.83 \pm 0.53) \times 10^{-10}$ exp[(−34.1 ± 2.1) kJ mol^{-1}/RT] cm^3 molecule^{-1} s^{-1} where the statistical uncertainties are 1σ. Confidence limits for k are ± 16%. Several isomers of C_4F_6H were characterized by ab initio methods. Below about 600 K the dominant pathway is suggested to be addition of H atoms to form $CF_2H-CF\bullet-CF=CF_2$ and/or $CF_2H-CF\bullet-CF=CF_2$. These adducts dissociate at elevated temperatures, and on the assumption that the major addition product at around 670 K is the more stable $CF_2H-CF\cdot$-$CF=CF_2$, the C−H bond dissociation enthalpy is estimated via a third-law method to be about −111 kJ mol^{-1}, with an estimated uncertainty of ± 7 kJ mol^{-1}.

1. Introduction

This paper describes the first kinetic studies of the reaction of atomic hydrogen with C_4F_6, perfluoro-1,3-butadiene or 1,1,2,3,4,4-hexafluoro-1,3-butadiene,

$$H + CF_2{=}CF{-}CF{=}CF_2 \rightarrow \text{products} \qquad (1)$$

and the overall rate constant k_1. This work was motivated by the possible application of C_4F_6 as a nonglobal warming fluorine precursor for plasma etching,[1,2] where reaction 1 may be significant when hydrogen species are present. Reaction 1 is a likely consumption path if the effluent stream is subject to incineration. C_4F_6 may also serve as a surrogate for perfluoroisobutene, a highly toxic product of incomplete fluorocarbon combustion,[3] in the context of the design of effective incineration processes.

As discussed below, the experiments reveal distinctly non-Arrhenius behavior, which we interpret in terms of a change in mechanism. At low temperatures addition of H atoms may create a substituted butenyl radical, a process that reaches equilibrium at higher temperatures so that the thermochemistry can be assessed. At even higher temperatures we speculate that an observed increase in the overall rate constant reflects fragmentation of the adduct to further products.

2. Experimental Section

Detailed descriptions of the experimental apparatus and modifications for H-atom detection have been given elsewhere.[4−7] The atomic H was produced by pulsed photolysis of NH_3 or H_2O in a large excess of C_4F_6 diluted in Ar bath gas by flash lamp radiation focused through a MgF_2 lens. The relative concentration of H atoms was monitored by time-resolved resonance fluorescence at the Lyman-α wavelength, 121.6 nm. This probe radiation was generated by a microwave-excited discharge lamp with a slow flow of 0.2% H_2 in Ar at about 0.27 mbar. The reaction zone is defined as the intersection of the photolysis and probe beams. Fluorescence from the reaction zone was detected with a solar-blind photomultiplier tube used with pulse counting and signal averaging. Typically 100−2000 fluorescence vs time profiles were accumulated at each set of conditions, with a repetition rate of 1−2 Hz. The temperature T of the gas in the reaction zone was measured before and after each set of measurements with a sheathed, unshielded thermocouple, corrected for radiation errors of up to 10 K, which is expected to be accurate (± two standard deviations, σ_T) to within 2%.[8] All experiments were carried out in a large excess of Ar bath gas at a total pressure P. The C_4F_6 and H-atom precursor (NH_3 or H_2O) concentrations were derived from P, T, the mole fractions of these species in Ar mixtures, and the gas flows measured with calibrated mass-flow controllers.

The H atoms reacted with C_4F_6 under pseudo-first-order conditions, [H] ≪ [C_4F_6], which implies an exponential decay of [H]:

$$d[H]/dt = -(k_1[C_4F_6] + k_{diff})[H] = -k_{ps1}[H]$$

$$[H] = [H]_0 \exp(-k_{ps1}t) \qquad (2)$$

where k_{diff} accounts for any loss of H atoms out of the reaction zone other than by reaction with C_4F_6, mainly via diffusion to the reactor walls, and at high temperatures, by reaction with the H-atom precursor,[9] as well as reaction with any photolysis fragments. The constant k_{ps1} was obtained by fitting the recorded fluorescence intensity I_f versus time t profile to an exponential decay over typically at least four lifetimes:

$$I_f = A[H] + B \qquad (3)$$

where A reflects the proportionality between [H] and the resonance fluorescence and B represents the constant contribution from scattered light in the system. Our fitting procedure for $I_f(t)$, which simultaneously determined the parameters $A[H]_0$, B, and k_{ps1} for each exponential decay, has been described

* Corresponding author e-mail: marshall@unt.edu.

10.1021/jp011546q CCC: $20.00
Published on Web 11/16/2001

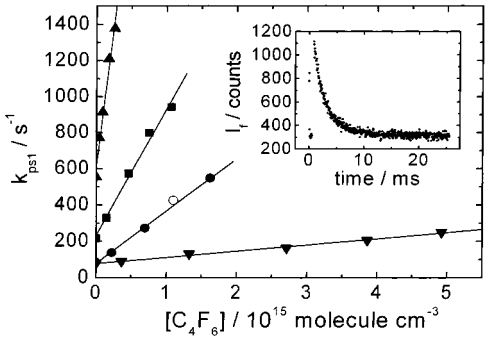

Figure 1. Plots of pseudo-first-order rate constant k_{ps1} vs $[C_4F_6]$. Downward triangles, 291 K; circles, 406 K; squares, 518 K; upward triangles, 1006 K. The inset shows the fluorescence decay corresponding to the open circle.

elsewhere,[10,11] and it propagates coupling between the parameters into the statistical error estimate for k_{ps1}. A check on the fit is that the value of B matches the signal measured before triggering the flash lamp. The second-order H + C_4F_6 rate constant k_1 was determined at a given set of conditions by linear fitting of k_{ps1} versus typically five values of $[C_4F_6]$. To verify that pseudo-first-order conditions were attained, the flash energy and precursor concentrations were varied to alter the initial radical concentrations. The reactants flowed through the reactor so that each flash lamp pulse photolyzed a fresh reaction mixture. The rate of sweeping gas through the reaction zone was slow compared to the reaction time scale of the H-atoms. The average gas residence time in the heated reactor before photolysis, τ_{res}, was varied to check for possible pyrolysis of C_4F_6.

3. Results

A typical exponential decay of fluorescence is shown in Figure 1, as are representative plots of k_{ps1} vs $[C_4F_6]$ over the temperature range studied, 290−1010 K. At zero reactant concentration the decays remained well-described by exponential fits, i.e., the kinetics remained effectively first-order. The linear fits to these plots of k_{ps1} vs $[C_4F_6]$ passed close to the k_{diff} measurement obtained with $[C_4F_6] = 0$, which ranged from 80 s^{-1} at low temperatures and high pressures to 870 s^{-1} at the highest temperature and low pressures. The slopes of 48 of these plots yield the k_1 values listed in Table 1, together with the statistical uncertainties. Good linearity in these plots leads to small σ_k/k values. These uncertainties σ_k are obtained from weighted fits to the plots of k_{ps1} vs $[C_4F_6]$, where the uncertainties in the exponential decay analysis and the propagated contributions from pressure, temperature, and flow, derived from our own calibrations and the instrument specifications, were taken into account. Also shown are the experimental parameters T, P, τ_{res}, the energy discharged in the flash lamp E, and the concentrations employed. As may be seen from Table 1, there is no significant variation of k_1 with E (typically varied by a factor of 2), or the concentration of the photolytic precursor (varied by up to a factor of 4). Although we do not obtain information about the absolute value of $[H]_0$, these two factors influence the initial radical concentrations. Figure 2, an Arrhenius plot of the k_1 data, shows that points with different $[H]_0$ and/or different precursors lie on the same curve. This indicates that pseudo-first order conditions were attained and that reaction 1 was successfully isolated from secondary chemistry involving photolytically or chemically produced species and any interaction between a precursor and C_4F_6. The independence of k_1 from τ_{res}, varied by a factor of 2−4, especially at the higher temperatures, shows that pyrolysis of C_4F_6 did not interfere.

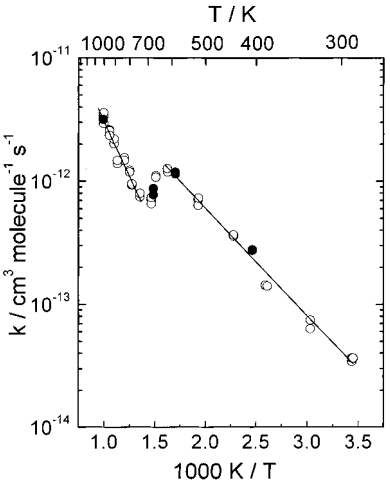

Figure 2. Arrhenius plot for the H + C_4F_6 reaction, showing 48 measurements made with NH_3 (open circles) and H_2O (solid circles) as H-atom precursors, and fits to the low and high-temperature data (solid lines).

There are clearly three regimes in Figure 2. A weighted Arrhenius fit to the data at $T < 620$ K, which takes σ_{k1} and σ_T into account, yields

$$k_1(T) = (3.40 \pm 0.34) \times 10^{-11} \times \exp[(-16.7 \pm 0.4)\ \text{kJ mol}^{-1}/RT]\ \text{cm}^3\ \text{molecule}^{-1}\ \text{s}^{-1} \quad (290\ \text{K} < T < 620\ \text{K}) \quad (4)$$

The quoted errors are 1σ and are statistical only. Consideration of the covariance leads to a 1σ precision for the fitted $k_1(T)$ of 3−6%. For flow systems, consideration of possible systematic errors in calibrations and measurements leads to an estimated accuracy of 10−15%.[12] Here we allow for ±10% and combine this in quadrature with the worst-case 2σ to derive a 95% confidence interval of ±16%.

A similar analysis of the high-temperature regime at $T > 700$ K leads to

$$k_1(T) = (1.83 \pm 0.53) \times 10^{-10} \times \exp[(-34.1 \pm 2.1)\ \text{kJ mol}^{-1}/\text{RT}]\ \text{cm}^3\ \text{molecule}^{-1}\ \text{s}^{-1} \quad (700\ \text{K} < T < 1010\ \text{K}) \quad (5)$$

with a 1σ precision of 3−6% for $k_1(T)$ and a 95% confidence interval, allowing for possible systematic errors, of ±16%.

In the intermediate regime, 660 K < T < 680 K, fluorescence decays remained approximately exponential and k_1 dropped rapidly with temperature, with an effective activation energy of about −84 kJ mol^{-1}. This regime is considered in more detail below.

4. Discussion

4.1. Low-Temperature Regime, T < 620 K. Under our conditions C−F bonds are essentially inert to direct H-atom attack (F-abstraction has a high energy barrier and the rate constant is less than 10^{-18} cm^3 $molecule^{-1}$ s^{-1} at 1000 K),[13] and a plausible path for reaction in the low-temperature regime is addition to a π bond followed by collisional stabilization.

TABLE 1: Rate Constant Measurements on the Reaction H + C_4F_6

T, K	*P*, mbar	τ_{res}, s	*E*, J	[precursor],[a] 10^{15} molecule cm^{-3}	k_{diff}, s^{-1}	[C_4F_6], 10^{14} molecule cm^{-3}	$k_1 \pm \sigma_{k_1}$, 10^{-13} cm^{-3} molecule^{-1} s^{-1}
290	69	6.4	3.6	2.6	76	3.63−46.8	0.363 ± 0.020
290	69	6.4	3.6	0.88	82	3.63−47.3	0.366 ± 0.020
291	136	6.6	2.0	1.8	77	3.68−49.1	0.342 ± 0.013
291	136	6.6	4.1	1.8	72	3.68−49.1	0.366 ± 0.030
330	141	5.9	4.1	1.4	79	3.43−21.1	0.635 ± 0.015
330	73	3.0	4.1	1.4	90	3.15−21.8	0.748 ± 0.023
383	71	2.6	4.1	0.60	98	2.78−18.4	1.41 ± 0.04
386	71	5.2	4.1	0.60	109	2.73−18.6	1.43 ± 0.07
406	133	4.5	4.1	1.1[b]	86	2.33−16.5	2.79 ± 0.07
406	68	2.2	4.1	1.1[b]	117	2.35−16.0	2.74 ± 0.03
439	68	2.1	4.1	0.49	141	2.23−15.4	3.58 ± 0.12
439	68	4.3	4.1	0.49	141	2.23−15.3	3.68 ± 0.06
518	56	1.5	2.0	0.67	216	1.53−10.7	7.33 ± 0.26
519	27	0.70	4.1	0.16	441	0.749−4.99	7.14 ± 0.18
519	27	0.70	2.0	0.16	431	0.749−4.99	6.40 ± 0.09
588	136	3.2	4.1	0.61[b]	105	1.67−11.4	11.5 ± 0.1
588	68	1.5	4.1	0.60[b]	210	1.64−11.2	11.9 ± 0.6
615	136	0.77	4.1	0.18	438	0.785−5.50	11.9 ± 0.7
617	68	1.6	4.1	0.18	243	0.816−5.66	12.7 ± 0.3
663	33	0.68	4.1	0.16	542	0.673−4.91	11.1 ± 0.2
663	71	1.5	4.1	0.17	311	0.869−5.37	10.8 ± 0.3
674	132	2.7	4.1	0.65[b]	129	1.45−9.77	7.78 ± 0.42
674	65	1.3	4.1	0.62[b]	263	1.34−9.30	8.75 ± 0.39
683	72	1.4	4.1	0.33	267	1.44−10.1	7.10 ± 0.39
683	33	1.3	4.1	0.16	510	0.715−4.99	6.58 ± 0.28
683	69	1.4	4.1	0.32	269	1.35−10.7	7.37 ± 0.22
740	67	1.3	4.1	0.15	293	0.733−4.63	7.48 ± 0.44
740	35	0.64	4.1	0.15	547	0.687−4.54	7.98 ± 0.38
786	35	0.60	4.1	0.14	654	0.646−4.28	9.34 ± 0.40
786	68	1.2	4.1	0.14	383	0.640−4.35	9.53 ± 0.09
800	136	2.4	4.1	0.28	102	1.38−8.71	12.3 ± 0.3
800	65	1.1	4.1	0.25	336	1.11−8.13	11.9 ± 0.2
834	136	2.2	4.1	0.52	138	1.17−8.42	15.6 ± 0.4
834	65	1.1	4.1	0.50	357	1.14−7.84	14.8 ± 0.2
885	68	1.0	4.1	0.28	358	1.86−7.64	14.8 ± 0.4
885	69	2.1	4.1	0.29	438	1.97−8.23	14.7 ± 0.3
885	35	0.53	2.0	0.29	771	0.815−3.88	13.9 ± 0.5
885	35	0.53	4.1	0.29	747	0.815−3.88	14.8 ± 0.1
911	69	1.0	4.1	0.47	395	1.03−7.50	20.2 ± 1.0
911	133	2.0	4.1	0.47	185	1.16−7.47	22.1 ± 0.4
949	68	1.0	4.1	0.12	504	0.583−3.63	26.1 ± 0.8
949	132	1.9	4.1	0.45	281	1.01−6.93	25.6 ± 1.3
949	69	1.0	4.1	0.46	426	1.04−7.28	23.6 ± 1.1
1006	33	0.50	4.1	0.21	548	0.481−1.94	33.8 ± 3.0
1006	67	0.90	4.1	0.21	895	0.537−2.92	29.5 ± 3.5
1006	129	1.8	4.1	0.83	553	0.470−2.72	34.0 ± 2.2
1006	65	1.8	4.1	0.80	285	0.454−2.63	36.0 ± 1.6
1011	53	0.94	4.1	0.58[b]	445	0.545−3.33	31.8 ± 1.8

[a] Unless noted, the H-atom precursor is NH_3. [b] H_2O used as H-atom source.

Two initial adducts are possible, corresponding to addition to a terminal or central carbon atom:

$$H + CF_2{=}CF{-}CF{=}CF_2\ (+Ar) \rightarrow CF_2H{-}CF\bullet{-}CF{=}CF_2\ (+Ar) \quad (1a)$$

$$H + CF_2{=}CF{-}CF{=}CF_2\ (+Ar) \rightarrow CF_2\bullet{-}CFH{-}CF{=}CF_2\ (+Ar) \quad (1b)$$

To make a qualitative assessment of which adduct is more likely, we have derived the geometries, vibrational frequencies and energies of the reactants, transition states, and adducts at the HF/6-31G(d) level of ab initio molecular orbital theory. Computations were carried out using the GAUSSIAN98 program.[14] The results are shown in Figure 3, Table 1S of the Supporting Information, and Table 2. Because of the modest basis set and, in some cases, significant degree of spin contamination ($\langle S^2 \rangle$ greater than the ideal value of 0.75, see Table 2), energies at the HF/6-31G(d) geometries were recalculated using density functional theory with a larger basis set, denoted B3LYP/6-311G(2df,p). As may be seen from Table 2, structure **2** is calculated to be about 60 kJ mol^{-1} more stable than structure **3**, in line with an argument that the radicals are electron deficient and the more substituted radical center is stabilized inductively by the substituents. There is a somewhat smaller barrier to addition to form **2** rather than **3**, i.e., the transition state **7** is calculated to lie about 3−14 kJ mol^{-1} below transition state **8**. These differences are not large and the B3LYP/6-311G(2df,p) data are unlikely to be quantitatively accurate, and we speculate that over much of the temperature range 290−620 K a mixture of both adducts may be formed.

Such addition reactions are in principle pressure-dependent when collisional stabilization of the initially excited adduct by the bath gas, Ar in our experiments, is rate limiting. We have investigated the likely pressure dependence of channel 1a via RRKM theory,[15] using the UNIMOL program.[16] The threshold

TABLE 2: Ab Initio Data for Species in the Reaction H + C_4F_6

	HF/6-31G(d)				B3LYP/6-311G(2df,p)		
species	energy[a]	ZPE[a]	$\langle S^2 \rangle$	enthalpy [b]	energy[a]	$\langle S^2 \rangle$	enthalpy [b]
H	−0.49823	0.00000	0.750		−0.50216	0.750	
C_4F_6 **1**	−747.99282	0.04347	0.000		−751.62943	0.000	
$CF_2H-CF\bullet-CF=CF_2$ **2**	−748.58821	0.05283	0.958	−233.1	−752.22266	0.776	−217.1
$\bullet CF_2-CFH\ -CF=CF_2$ **3**	−748.56748	0.05508	0.756	−173.4	−752.20028	0.752	−153.2
$\bullet CFH-CF_2\ -CF=CF_2$ **4**	−748.56665	0.05375	0.760	−174.4	−752.19837	0.753	−151.2
$CF_2H-CF_2-C\bullet=CF_2$ **5**	−748.58007	0.05526	0.916	−206.0	−752.19830	0.758	−147.5
$CF_3-CH\bullet-CF=CF_2$ **6**	−748.62413	0.05248	0.950	−328.2	−752.25134	0.774	−293.3
$H\cdots CF_2-CF\bullet-CF=CF_2$ TS **7**	−748.48306	0.04224	1.275	18.1	−752.12751	0.780	7.8
$\bullet CF_2-CF(\cdots H)-CF=CF_2$ TS **8**	−748.48206	0.04224	1.385	20.8	−752.12205	0.811	22.1
2 ↔ 3 isomerization TS **9**	−748.45936	0.04703	1.008	91.5	−752.12018	0.771	38.3

[a] In au. 1 au ≈ 2625 kJ mol^{-1}. ZPE is unscaled. [b] 0 K value in kJ mol^{-1}, relative to H + C_4F_6.

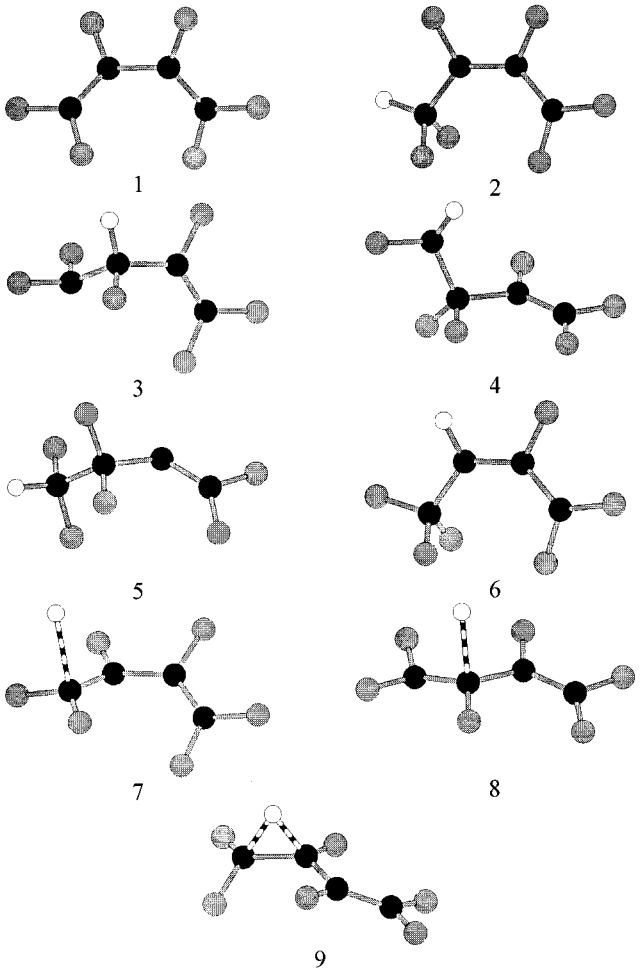

Figure 3. Geometries for C_4F_6, five C_4F_6H isomers and two transition states for H + C_4F_6 addition, calculated at the HF/6-31G(d) level of theory. **1** C_4F_6; **2** $CF_2H-CF\bullet-CF=CF_2$; **3** $\bullet CF_2-CFH-CF=CF_2$; **4** $\bullet CFH-CF_2-CF=CF_2$; **5** $CF_2H-CF_2-C\bullet=CF_2$; **6** $CF_3-CH\bullet-CF=CF_2$; **7** $H\cdots CF_2-CF\bullet-CF=CF_2$ TS; **8** $\bullet CF_2-CF(\cdots H)-CF=CF_2$ TS.

energy for dissociation of the adduct was set to be 123 kJ mol^{-1} (this value includes the bond strength, see later, plus an energy barrier to match the activation energy in the reverse direction, eq 4), and its Lennard-Jones parameters were assumed to be similar to those for C_4F_6: $\sigma = 5.9 \times 10^{-10}$ m based on additive atomic volume increments[15] and $\epsilon/k_B = 340$ K based on the boiling temperature[15] of 280 K.[17] For simplicity all internal degrees of freedom in the adduct **2** and TS **7** were treated as vibrations in the RRKM calculations, and, because we deal with a tight transition state close to the high-pressure limit, overall rotations were not separated into active and inactive modes. The results suggest that at 290 K the falloff pressure, defined as the pressure P where $k_{1a}(P)/k_{1a}(P=\infty) = 1/2$, is less than 0.1 mbar of Ar, so the present measurements are essentially at the high-pressure limit. The corresponding preexponential factor for recombination was calculated to be 3.3×10^{-11} cm^3 molecule^{-1} s^{-1} at 298 K, which is very close to the measured value in eq 4.

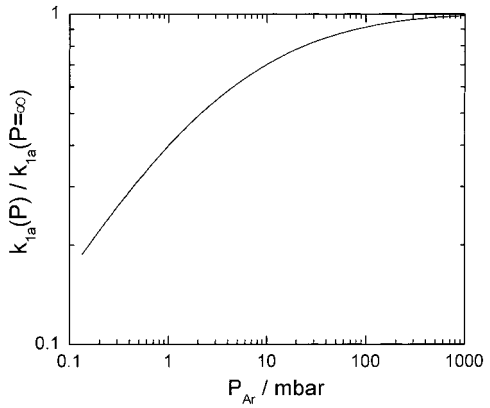

Figure 4. Fall off for addition of H to C_4F_6 derived via RRKM theory (see text) at 620 K.

At 620 K, with $\langle \Delta E_{down} \rangle = 493$ cm^{-1}, the falloff pressure is around 2.5 mbar of Ar and the present work, conducted at higher pressures (see Table 1), is in the falloff regime but close to the high-pressure limit, as illustrated in Figure 4. The predicted pressure dependence would be small, with the RRKM values of k_{1a} at 68 and 136 mbar changing by only 4%, consistent with the lack of observed systematic variation with P. At this temperature the measured recombination rate constants are predicted to lie around 5−10% below the high-pressure limiting values.

We note that our measurements yield a substantial positive activation energy for a recombination reaction, (1a) and/or (1b), of about 17 kJ mol^{-1}, which is somewhat larger than that observed for H + π-bonded carbon in simple hydrocarbon systems. For comparison, H + ethylene has $E_a \approx 9$ kJ mol^{-1} in the high-pressure limit at 298 K.[18] The computational results in Table 2 confirm the presence of significant barriers along both H-atom addition pathways.

A 1,2 hydrogen shift would lead to isomerization between the adducts **2** and **3**. We have investigated this possibility computationally and characterized the transition state **9** for this process (see Figure 3 and Table 2). Apparently the geometry constraints of the 1,2 shift lead to bonding by H to the carbon atoms at unfavorable angles, and the high barrier means that dissociation rather than isomerization is the more likely fate of the adducts.

4.2. High-Temperature Regime, *T* > 700 K. As noted in the previous section, direct attack by H on a C−F bond seems

unlikely. We speculate that an addition-fragmentation mechanism may operate at high temperatures:

$$H + C_4F_6 \leftrightarrow \text{adduct} \rightarrow \text{fragments} \quad (6)$$

where the overall observed rate constant, summarized by eq 5, is the product of the concentration equilibrium constant for adduct formation K_c, equal to the ratio of forward and reverse rate constants, and the rate constant for adduct fragmentation, defined here as k_6. The nature of the fragments is unknown. We note that fission of the central C−C bond of structure **3** would lead to the perfluorovinyl radical C_2F_3 and the stable trifluoroethylene molecule, C_2F_3H. Similarly, structure **2** could lead to the same products if C−C fission is concerted with a 1,2 hydrogen atom shift. Combination of Δ_fH_{298} for these two fragments, −220[19] and −474 ± 8.4 kJ mol^{-1},[20] respectively, with $\Delta_fH_{298}(H) = 218$ kJ mol^{-1} and $\Delta_fH_{298}(C_4F_6) = -942$ kJ mol^{-1},[20] yields an overall reaction enthalpy for reaction 6 of $\Delta H_{298} = 30$ kJ mol^{-1}. This endothermicity compares well with the measured activation energy of 34 kJ mol^{-1}, although there is considerable uncertainty in ΔH_{298}, which we guess to be at least 20 kJ mol^{-1}. The accord does not mean the fragments are uniquely identified, but it indicates that the general scheme of eq 6 is plausible. Analogous products, with F replaced by H, were proposed for the high-temperature reaction of H with butadiene by Benson and Haugh.[21]

4.3. Intermediate Temperature Regime, 660 K < *T* < 680 K. We suggest that the abrupt drop in the overall rate constant k_1 is caused by adduct formation coming to equilibrium. As the temperature is raised close to the point where H-atom addition becomes thermodynamically unfavorable, only the most stable adduct **2** will be formed. Isomer **3** will dissociate more quickly and not contribute to net loss of H atoms here. The rate constant k_{-1a} for the endothermic dissociation of **2** has a large activation energy, so that at slightly higher temperatures the reverse of 1a becomes significantly faster and H is no longer consumed via channel 1a. Over a narrow temperature range both adduct formation and dissociation are comparable. Over this range we consider the following mechanism quantitatively:

$$H + CF_2{=}CF{-}CF{=}CF_2 \rightarrow \text{adduct} \quad k_{1a}$$

$$\text{adduct} \rightarrow H + CF_2{=}CF{-}CF{=}CF_2 \quad k_{-1a}$$

$$\text{adduct} \rightarrow \text{products (excluding H)} \quad k_6$$

$$H \rightarrow \text{loss} \quad k_{\text{diff}}$$

Solution of the rate equations via the Laplace transform method yields

$$[H] = [H]_0 \frac{(k_{-1a} + k_6 + \lambda_1)e^{\lambda_1 t} - (k_{-1a} + k_6 + \lambda_2)e^{\lambda_2 t}}{\lambda_1 - \lambda_2} \quad (7)$$

where

$$\lambda_{1,2} = \frac{-(k_{1a}[C_4F_6] + k_{-1a} + k_6 + k_{\text{diff}}) \pm \sqrt{(k_{1a}[C_4F_6] + k_{\text{diff}} - k_{-1a} - k_6)^2 + 4k_{1a}k_{-1a}[C_4F_6]}}{2} \quad (8)$$

Fluorescence decays were again fit to the form of eq 3, where now [H] is described by eqs 7−9. There are only three variables to be adjusted in this fitting: A, B, and k_{-1a}, and these were varied directly to minimize the root-mean-square deviations between observed decays and eq 7. An example is shown as the inset of Figure 5, and we were intrigued to see how an apparently exponential decay could be well represented as a biexponential, eq 7. The other parameters were found as follows: k_{1a} was obtained via a short upward extrapolation of eq 4 while k_6 was derived from a short downward extrapolation of eq 5, coupled with application of the scheme shown in eq 6, i.e., $k_1(T)$ for $T > 700$ K $= K_c k_6$, so that

$$k_6 = \frac{k_1(T;T > 700\text{K})k_{-1a}}{k_{1a}} \quad (9)$$

, and k_{diff} was obtained from decays with zero reactant concentration.

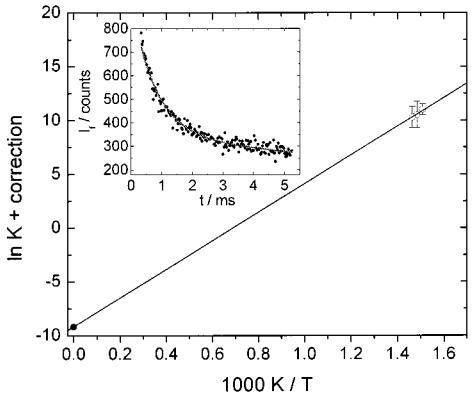

Figure 5. van't Hoff plot for addition of H to C_4F_6. The intercept is constrained to the statistical mechanical value of $\Delta S_{298}/R$ (see text). The inset shows a typical fluorescence decay obtained at 674 K together with a biexponential fit (see text, eq 7).

TABLE 3: Thermochemical Information for Adduct Formation between H and C_4F_6

T, K	no. decays	K_c [a] ± σ_{Kc}, 10^{-15} cm^3 molecule^{-1}	ln K[b] ± $\sigma_{\ln K}$
663	8	3.85 ± 0.84	10.62 ± 0.24
674	8	2.77 ± 1.44	10.13 ± 0.62
683	12	2.10 ± 1.11	9.88 ± 0.50

[a] Mean and standard deviation of K_c. [b] Mean and standard deviation of ln K.

The results of this kinetic analysis are summarized in Table 3. The concentration equilibrium constant for adduct formation K_c equals k_{1a}/k_{-1a}, and from this we calculated the equilibrium constant K, which is dimensionless and is defined relative to a standard state of unit activity for 10^5 Pa. The temperature variation of K contains thermochemical information. Because of the short temperature range we employ a "third-law" analysis, illustrated in Figure 5. This is a van't Hoff plot where the intercept is fixed at the statistical mechanical value of $\Delta S_{298}/R = -9.17$ J K^{-1} mol^{-1} for channel 1a. Statistical mechanics were also employed to derive the temperature variation of ΔS and ΔH, to obtain the correction added to ln K in Figure 5, equal to about 0.4:

$$\ln K + \text{correction} = \Delta S_{298}/R - \Delta H_{298}/RT \quad (10)$$

where

$$\text{correction} = -(\Delta S_T - \Delta S_{298})/R + (\Delta H_T - \Delta H_{298})/RT \quad (11)$$

Ab initio input data were taken from Table 1S, and corrections were included for hindered internal rotors in the reactants and

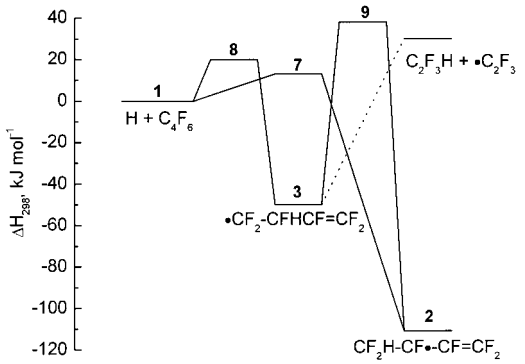

Figure 6. Schematic diagram of approximate relative enthalpies at 298 K for reactants, transition states, and possible products in the H + C_4F_6 reaction, obtained from experiment where possible, or otherwise by ab initio calculations.

products identified via the algorithm of Ayala and Schlegel,[22] as implemented within GAUSSIAN98.[14] The slope of Figure 5 yields $\Delta H_{298} = -111$ kJ mol^{-1} for reaction 1a, with an estimated uncertainty of ± 7 kJ mol^{-1} based on the 2σ error bars for ln K. This is minus the bond dissociation enthalpy (BDE_{298}) for the adduct, and, for comparison, the BDE_{298} in the ethyl radical (leading to the analogous products H + CH_2=CH_2) is 150.2 $\pm$ 0.9 kJ mol^{-1}.[23] Apparently the electronegative substituents in the perfluorobutadiene system destabilize the radical adduct and/or the limited conjugation between the two π bonds in the reactant is lost upon addition of an H atom. The conjugation in C_4F_6 is only partial because the lowest energy configuration is nonplanar: steric repulsions between the terminal CF_2 groups lead to a dihedral angle along the carbon backbone of 53° rather than zero.

We stress that the above analysis depends on the correctness of the assumed mechanism. Sato and co-workers have drawn attention to the facile 1,2 migration of F atoms in chemically activated fluoroethyl radicals.[24,25] If such processes occur in the present system, then three further isomers of C_4F_6H would be accessible and geometries of **4**, **5**, and **6** are shown in Figure 3. Table 2 indicates that **4** and **5** are less stable than **2** and **3** and therefore are not important, and that isomer **6** is the most stable of all. The greater density of states in the larger systems studied here will tend to make such isomerization less important, but we cannot rule it out completely.

5. Conclusions

The kinetic measurements reveal distinct non-Arrhenius behavior for the reaction of H with C_4F_6, whose rate constant increases up to 620 K, then drops, then increases again above about 700 K. These results can be rationalized in terms of a low-temperature addition channel, which comes to equilibrium at around 670 K, with a fragmentation pathway becoming important at higher temperatures. A fit to the kinetic data in the equilibration region yields the bond dissociation enthalpy in the more stable adduct, which density functional calculations suggest is $CF_2H-CF\bullet-CF=CF_2$. Figure 6 summarizes the results of this study schematically and shows the relative energies of reactants, transition states, and products obtained via experiment and/or calculation.

Acknowledgment. We thank Dr. Ashutosh Misra for his help and encouragement. This was work was supported by the R. A. Welch Foundation (Grant B-1174), Air Liquide Electronic Chemicals & Services, Inc., and the UNT Faculty Research Fund, and we gratefully acknowledge use of an SGI Origin 2000 computer at the National Center for Supercomputing Applications (Grant CHE000015N).

Supporting Information Available: Table 1S summarizes Cartesian coordinates, rotational constants and vibrational frequencies for reactants and possible products in the H + C_4F_6 reaction, calculated at the HF/6-31G(d) level of theory. This material is available free of charge via the Internet at http://pubs.acs.org.

References and Notes

(1) Hung, H. R.; Caulfield, J. P.; Shan, H.; Wang, R.; Yin, G. Z. Oxide etch process using hexafluorobutadiene and related unsaturated hydrocarbons. U.S. Patent 6,174,451, 2001.

(2) Chatterjee, R.; Karecki, S.; Pruette, L.; Reif, R. *Proc. Electrochem. Soc.* **2000**, *99*−*30*, 251.

(3) Tsang, W.; Burgess, D. R., Jr.; Babushok, V. *Combust. Sci. Technol.* **1998**, *139*, 385.

(4) Shi, Y.; Marshall, P. *J. Phys. Chem.* **1991**, *95*, 1654.

(5) Ding, L.; Marshall, P. *J. Phys. Chem.* **1992**, *96*, 2197.

(6) Goumri, A.; Yuan, W.-J.; Ding, L.; Shi, Y.; Marshall, P. *Chem. Phys.* **1993**, *177*, 233.

(7) Peng, J.; Hu, X.; Marshall, P. *J. Phys. Chem. A* **1999**, *103*, 5307.

(8) Ding, L.; Marshall, P. *J. Chem. Soc., Faraday Trans.* **1993**, *89*, 419.

(9) Ko, T.; Marshall, P.; Fontijn, A. *J. Phys. Chem.* **1990**, *94*, 1401.

(10) Marshall, P. *Comput. Chem.* **1987**, *11*, 219.

(11) Marshall, P. *Comput. Chem.* **1989**, *13*, 103.

(12) Howard, C. J. *J. Phys. Chem.* **1979**, *83*, 3.

(13) Berry, R. J.; Ehlers, C. J.; Burgess, D. R., Jr.; Zachariah, M. R.; Marshall, P. *Chem. Phys. Lett.* **1997**, *269*, 107.

(14) Frisch, M. J.; Trucks, G. W.; Schlegel, H. B.; Scuseria, G. E.; Robb, M. A.; Cheeseman, J. R.; Zakrzewski, V. G.; Montgomery, J. A., Jr.; Stratmann, R. E.; Burant, J. C.; Dapprich, S.; Millam, J. M.; Daniels, A. D.; Kudin, K. N.; Strain, M. C.; Farkas, O.; Tomasi, J.; Barone, V.; Cossi, M.; Cammi, R.; Mennucci, B.; Pomelli, C.; Adamo, C.; Clifford, S.; Ochterski, J.; Petersson, G. A.; Ayala, P. Y.; Cui, Q.; Morokuma, K.; Malick, D. K.; Rabuck, A. D.; Raghavachari, K.; Foresman, J. B.; Cioslowski, J.; Ortiz, J. V.; Stefanov, B. B.; Liu, G.; Liashenko, A.; Piskorz, P.; Komaromi, I.; Gomperts, R.; Martin, R. L.; Fox, D. J.; Keith, T.; Al-Laham, M. A.; Peng, C. Y.; Nanayakkara, A.; Gonzalez, C.; Challacombe, M.; Gill, P. M. W.; Johnson, B.; Chen, W.; Wong, M. W.; Andres, J. L.; Gonzalez, C.; Head-Gordon, M.; Replogle, E. S.; Pople, J. A. GAUSSIAN 98; Rev A.6.; Gaussian Inc.: Pittsburgh, 1998.

(15) Gilbert, R. G.; Smith, S. C. *Theory of Unimolecular and Recombination Reactions*; Oxford University Press: Oxford, 1990.

(16) Gilbert, R. G.; Jordan, M. J. T.; Smith, S. C. UNIMOL; Sydney, Australia, 1990, (see preceding ref).

(17) *PCR Research Chemicals Catalog*; PCR Inc.: Gainesville, FL, 1988.

(18) Baulch, D. L.; Cobos, C. J.; Cox, R. A.; Frank, P.; Hayman, G.; Just, T.; Kerr, J. A.; Murrells, T.; Pilling, M. J.; Troe, J.; Walker, R. W.; Warnatz, J. *J. Phys. Chem. Ref. Data* **1994**, *23*, 847.

(19) Haworth, N. L.; Smith, M. H.; Backsay, G. B.; Mackie, J. C. *J. Phys. Chem. A* **2000**, *104*, 7600. The disagreement between experiment and theory for C_2F_3 is the largest of any species in this study, although not discussed. We have selected the Gaussian-3/isodesmic value as the most reliable.

(20) Afeefy, H. Y.; Liebman, J. F.; Stein, S. E. Neutral Thermochemical Data. In *NIST Chemistry WebBook, NIST Standard Reference Database Number 69*; Mallard, W. G., Linstrom, P. J., Eds.; NIST: Gaithersburg, MD, 2000.

(21) Benson, S. W.; Haugen, G. R. *J. Phys. Chem.* **1967**, *71*, 1735.

(22) Ayala, P. Y.; Schlegel, H. B. *J. Chem. Phys.* **1998**, *108*, 2314.

(23) Brouard, M.; Lightfoot, P. D.; Pilling, M. J. *J. Phys. Chem.* **1986**, *90*, 445.

(24) Kohida, T.; Kotaka, M.; Sato, S.; Ishida, T.; Yamamoto, K.; Yamazaki, T.; Kitazume, T. *Bull. Chem. Soc. Jpn.* **1987**, *60*, 3131.

(25) Kotaka, M.; Sato, S.; Shimokoshi, K. *J. Fluorine Chem.* **1987**, *37*, 387.